18

Preparation of Hollow Titanium Dioxide Shell Thin Films from Aqueous Solution of Ti-Lactate Complex for Dye-Sensitized Solar Cells

Masaya Chigane, Mitsuru Watanabe and Tsutomu Shinagawa
Osaka Municipal Technical Research Institute
Japan

1. Introduction

As photovoltaic devices possessing potential for low processing costs and flexible architectures, dye-sensitized solar cells (DSSCs) using nanocrystalline TiO_2 (nc-TiO_2) electrodes have been extensively studied.(Bisquert et al., 2004; O'Regan & Grätzel, 1991) Congruently with increasingly urgent dissemination of solar cells against crisis of a depletion of fossil fuel, DSSCs are as promising alternative to conventional silicon-type solar cells. The main trend of investigations of DSSCs originates from the epoch-making works by Grätzel and co-workers in the early 1990s. (O'Regan & Grätzel, 1991) A typical construction of the cells are composed of dye-molecules (usually Ru complexes) coated nc-TiO_2 electrodes on transparent-conductive (TC) backcontact (usually fluorine-doped tin oxide (FTO)) glass substrate and counter Pt electrodes sandwitching triiodine/iodine [I_3^-/I^-] redox liquid electrolyte layer maintaining electrical connection with the counter Pt electrode. The voids of the network of TiO_2 nanoparticles connection form nanopores which are efficiently filled with electrolyte solution. An operation mechanism of DSSC begins with harvesting incident light by dye-molecules via photoexcitation of electron from the highest occupied molecular orbital (HOMO) to the lowest unoccupied molecular orbital (LUMO). The photoexcited electrons are transferred to the conduction band of the nc-TiO_2 and diffuse in TiO_2 matrix to TC layer followed by ejection to outer electric load. The oxidized dye is reduced by the electrolyte (I^-) and the positive charge is transported to Pt counter electrode. As well as close fitting of photo-absorption spectra of dyes to the spectrum of sunlight mainly in visible light region (nearly panchromatic dyes) (Nazeeruddin et al., 2001) the strong dye-TiO_2 coupling leading to rapid electron transfer from excited dye to TiO_2 (Tachibana et al., 1996) realizes practically promising solar-to-electrical conversion efficiency: more than 10 %. The charge separation of DSSCs occurs at the interface TiO_2 nanoparticles / dye molecules / [I^-/I_3^-] electrolyte. Therefore the combination of Ru-complex and TiO_2 is currently almost ideal choice in DSSC. Some problems of the TiO_2 nanoparticles electrode, however, remain room to investigate. Connection points of TiO_2 nanoparticles decrease an effective area of interface, and play a role on electron scattering sites, leading to restrict the conversion efficiency.(Enright & Fizmaurice, 1996; Peng et al., 2003) Though denser films seemingly improve the electron migration, they result in decrease of surface area for dye adsorption. Additionally TiO_2 nanoparticles electrodes are

usually prepared by embrocation methods, e. g., a squeegee method, whereas via these methods great amount of Ti resource is consumed.
For the settlement several nanostructures of TiO_2 electrodes for DSSCs containing the array of nanorods,(Kang et al., 2008) nanotubes (Kang et al., 2009; Paulose et al., 2008) and assembly of spherical hollow (Kondo et al., 2006) or hemispherical (Yang et al., 2008) shells particles have been proposed owing to their ordered structures leading to ordered electron transport and large surface area for small amount of titanium as depicted in Fig. 1.

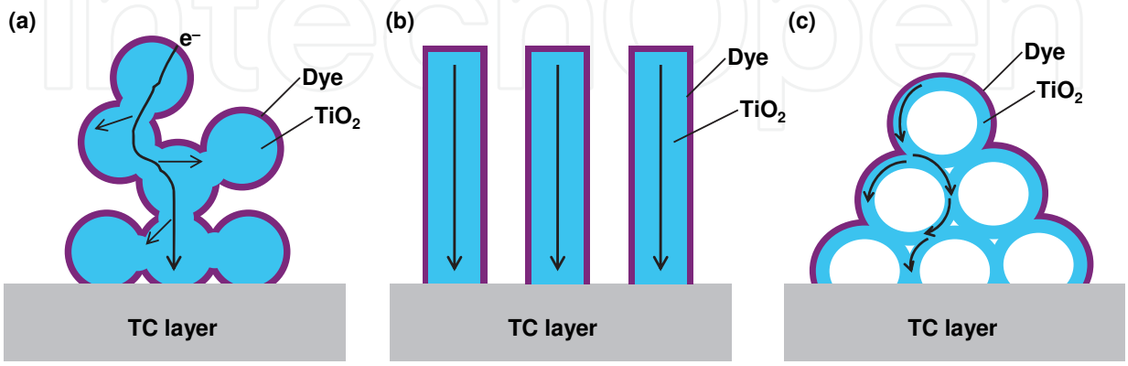

Fig. 1. Models of TiO_2 nano-structure electrode for DSSCs, (a) standard nanocrystalline particles, (b) nano tube or nano pillar arrays and (c) hollow shells.

Some works on ordered and multilayered hollow TiO_2 shells, which are inverse opal structure, have shown photonic crystalline effects leading to red shift in incident photon-to-current conversion efficiency (IPCE). (Nishimura et al., 2003; Yip et al., 2008) Recently energy conversion efficiencies of DSSCs using inverse TiO_2 opal, including 1.8 %, (Guldin et al., 2010) 3.47 % (Kwak et al., 2009) and 4.5 % (Qi et al., 2009) have been reported. In the previous work we prepared hollow TiO_2 shell monolayer films by the electrolysis of an aqueous $(NH_4)_2TiF_6$ solution on complicated polystyrene (PS) particles-preadsorbed substrate followed by calcination. (Chigane et al., 2009) Among few papers (Karuppuchamy et al., 2001; Yamaguchi et al., 2005) reporting the electrolytic preparation of TiO_2 for DSSC anode, the previous work first reported the DSSC conversion efficiency (0.63 %) using TiO_2 film prepared via electrolysis to our knowledge. From standpoint of methodology for a preparation of TiO_2 films electrolyses (electrodeposition) from aqueous solutions are a low cost and low resource consuming fabrication techniques since the deposition reaction occurs only nearby substrate. The $(NH_4)_2TiF_6$ solution is stable for long term, being able to undergo repeated electrolyses. However some industrial problems: liberation of highly toxic F^- during electrochemical deposition reaction leading to bad working environment. Moreover insufficient conversion efficiency calls multilayered hollow structures. As a water-soluble and environment-benign titanium compound titanium bis(ammonium lactato)dihydroxide (TALH) increasingly attracts attention. (Caruso et al., 2001; Rouse & Ferguson, 2002) Especially Ruani and co-workers (Ruani et al., 2008) have developed single-step preparation of PS-TALH core-shell precursor from a suspension containing both PS and TALH, followed by fabrication inverse opal TiO_2 films by calcination. The process seems to be simple and time-saving compared with other conventional methods: PS template followed by infiltration of Ti oxides or Ti compounds sol. (Galusha et al., 2008; King et al., 2005; Liu et al., 2010; Nishimura et al., 2002) However DSSC electrode properties of the film have not been

evaluated. There assumably are two reasons that the films becomes noncontiguous by calcination owing to drastic volume change from Ti-lactate to oxide and that H-TiO_2 film are difficult to be prepared in wide area. The latter problem is mainly due to aninonic surface functional groups of PS in usual cases despite electrostatically repulsive Ti-lactate anion leading to difficult formation of homogeneous structure. Based upon these trend and problems we propose in the present article some preparation methods of three-dimensional assembly of H-TiO_2 shells being applied to DSSC. Figure 2 illustrates our preparation process of H-TiO_2 shell films.

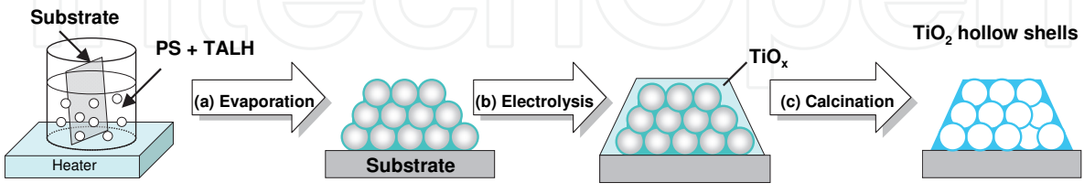

Fig. 2. Schematic representation of preparation process of hollow TiO_2 shell film.

The immersion of substrate in the initial suspension which contains both PS and TALH, followed by evaporation of water, forms a PS template coated with TALH (PS-TALH) precursor (Fig. 2 (a)). So as to avoid the volume change of films we supported the PS-TALH by electrodeposition of titanium oxide (TiO_x) thin film (Fig. 2(b)) thereon. The novelty of this method includes i) employing non-toxic TALH and PS with cationic surface groups which are supposedly good affinity with each other and ii) electrolysis of TALH solution for TiO_x coverage. As a whole, this article highlights a low cost, facile and soft fabrication process of hollow TiO_2 (H-TiO_2) shell films and aggressive participation of them in DSSC as a trendy nano-architechtural electrode.

2. Experimentals

Two types of PS possessing anionic (A-PS) and cationic (C-PS) functional group on the surface, prepared by an emulsifier-free emulsion polymerization of styrene monomer with potassium persulfate (KPS) and 2,2′-azobis(2-methylpropionamidine) dihydrochloride (AIBA) as a radical initiator, respectively, were used.(Watanabe et al., 2007) From SEM observations a diameter of A-PS and C-PS beads was ca. 400 nm and ca. 300 nm, respectively. A TC glass plate coated with fluorine-doped tin oxide (FTO, 10 Ω/square, ASAHI GLASS Co., Ltd, A11DU80) and quartz glass plate (1 mm of thickness) were used as substrates. As pretreatments of substrates, FTO (15 mm × 20 mm) was degreased by anodic polarization (+5 mA cm^{-2}) against Pt counter electrode for 30 s in a 1 mol dm^{-3} NaOH and quartz glass plate (20 mm × 40 mm) was immersed in a 10 % NaOH solution for 10 min at 333 K. Both substrates were thoroughly rinsed with deionized water and immersed in the colloidal suspension of PS and TALH in a cylindrical glass bottle being bent backward at about 60° against bottom. (Hartsuiker & Vos, 2008; Ye et al., 2001) The glass bottle containing the suspension and substrate was placed on a hot plate the temperature of surface of which was set at 345 K. In this way the temperature of the suspension was maintained at 325 K for 5–24 h until complete evaporation of water. The initial concentrations of PS and TALH in the suspension were 0.28 % and 0.0025 or 0.005 mol dm^{-3}, respectively. Hollow shells TiO_2 (H-TiO_2) films were formed by the calcinations of the PS-TALH precursor at 723 K for 1 h. In the calcination, the temperature was raised in rate of 2 h

from room temperature to 723 K. In some cases TiO_x films were electrodposited on the PS-TALH precursor films before calcination by a cathodic electrolysis in the electrolyte solution containing a 0.05 mol dm^{-3} TALH (Aldrich; reagent grade) and a 0.1 mol dm^{-3} NH_4NO_3 at –2 mA cm^{-2} of current density for 6 C cm^{-2} of charge density.

X-ray diffraction (XRD) patterns of the films in 3 cm^2 of deposition area were recorded on a RIGAKU RINT 2500 diffractometer (Cu Kα; λ = 0.1541 nm; 40 kV; 100 mA), with the incident angle (θ) fixed at 1°, scanning the diffraction angle (2θ) stepwise by 0.05° with a counting time of 10 s.

Transmission spectra and relative diffuse reflection (DR) spectra in ultraviolet (UV)–visible range of hollow shells were measured by means of Shimadzu UV-3150 spectrometer. An integral spherical detector equipment (Shimadzu ISR-3100) was used for DR spectroscopy with $BaSO_4$ powder (Wako Pure Chemical Industries) as a reference reflector. For the powder sample the hollow shell film was detached from quartz glass substrate by scratching with spatula.

X-ray photoelectron (XP) spectra of the films were obtained by means of Kratos AXIS-ULTRA DLD. A monochromated Al Kα (1486.6 eV; 150 W) line was used as the X-ray source. The pressure in the analyzing chamber was lower than < 1×10^{-8} Torr during measurements. Binding energies of Ti 2p and O 1s photoelectron peaks were corrected from the charge effect by referencing the C 1s signal of adventitious contamination hydrocarbon to be 284.8 eV.

For DSSC measurements, a composite TiO_2 (C-TiO_2) film composed of flat bottom TiO_2 layer and hollow shell film was prepared. The deposition area, corresponding to an active area of the cell, was adjusted to be 0.25 cm^2 using a mask. Initially TiO_x film was galvanostatically electrodeposited on the FTO in the electrolyte solution containing a 0.05 mol dm^{-3} TALH (Aldrich; reagent grade) and a 0.1 mol dm^{-3} NH_4NO_3 at –3 mA cm^{-2} of current density for 10 C cm^{-2} of charge density as a blocking layer of DSSC electrode. On the FTO/TiO_x layer the PS-TALH precursor was coated from aqueous suspension of 0.28 % C-PS and 0.0025 mol dm^{-3} TALH and thereon TiOx was coated by electrolysis. The TiO_2 hollow films on FTO substrates were immersed in an ethanolic solution of 0.3 mmol dm^{-3} ruthenium dye (bistetrabutylammonium cis-di(thiocyanato)-bis(2,2'-bipyridine-4-carboxylic acid, 4'-carboxylate ruthenium(II), Solaronix N719) for 14–16 h at room temperature. An electrolyte solution for DSSC was composed of 0.1 mol dm^{-3} LiI, 0.05 mol dm^{-3} I_2, 0.6 mol dm^{-3} 1,2-dimethyl-3-propylimidazolium iodine (DMPII, Solaronix) and 0.5 mol dm^{-3} 4-tert-butylpyridine in acetonitrile. A platinum-coated glass substrate was used for a counter electrode. The dye-coated TiO_2 electrode and the counter electrode were set sandwiching a separation polymer sheet (25 μm of thickness; Solaronix SX-1170) and the electrolyte. Photovoltaic current density (J)-voltage (V) curves were obtained using an instrument for the measurements of solar cell parameters (Bunkoh-Keiki Co., Ltd K0208, with a Keithley 2400) with photoirradiation by a 150 W xenon lamp under the condition that was simulated airmass 1.5 solar irradiance with the intensity of 100 mW cm^{-2}. Incident photon-to-electron conversion efficiency (IPCE) spectra ranging 400 to 800 nm of wavelength were measured by means of a spectral photosensitivity measurement system (Bunkoh-Keiki) with a 150 W xenon lamp light source. Calibration was performed using a standard silicon photodiode (Hamamatsu Photonics, S1337-1010BQ).

As a reference sample, TiO_2 nanocrystalline particles (nc-TiO_2) electrode prepared by a squeegee method from TiO_2 colloidal solution (Solaronix Ti-Nanoxide D) and calcination in the same way as the hollow films was subjected to DSSC measurements.

The area density: amount of deposited TiO_2 against area (mg cm^{-2}) was determined using an X-ray fluorescent spectrometer (Rigaku RIX3100).

3. Results and discussion

3.1 Characterization of H-TiO_2 films

Figure 3 shows SEM photographs of PS-TALH precursors. For both A-PS and C-PS, the sizes of spherical PS-TALH units appeared to be almost same as PS itself and core/shell structures of PS/TALH were not clearly observed as shown in expanded images (Fig. 3(b) and (d)). Some bulgy junctions between adjacent spheres, however, suggest accumulation of TALH. From appearance with eyes and SEM images, PS particles and TALH were uniformly mixed.

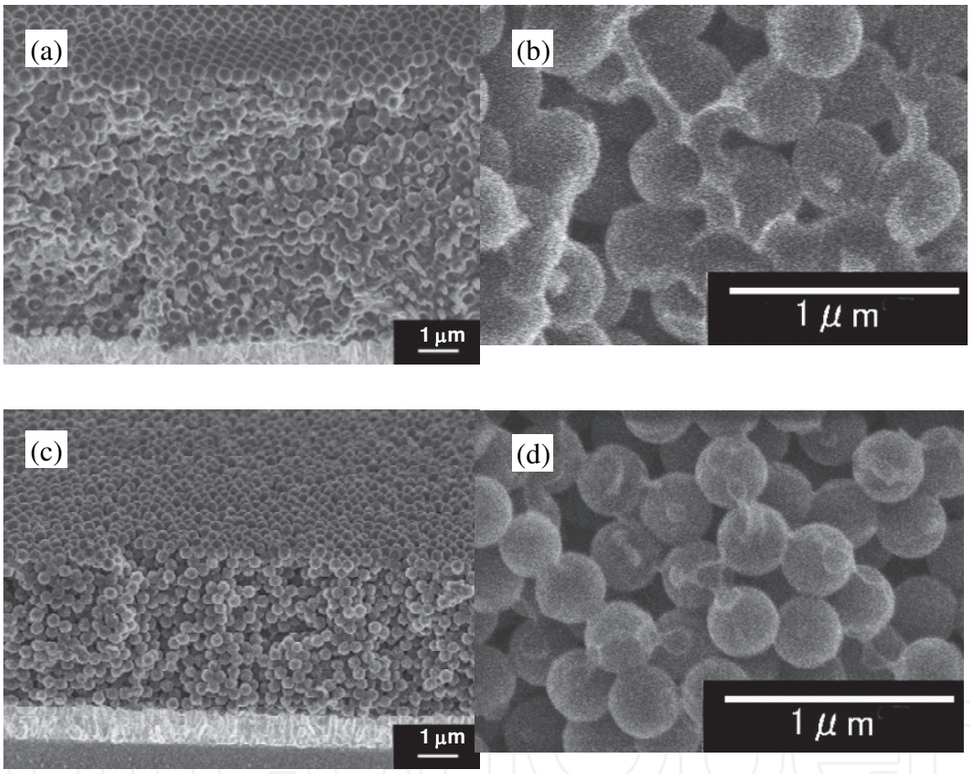

Fig. 3. Cross-sectional SEM photographs of PS-TALH films on FTO substrates from (a) or (b) A-PS and (c) or (d) C-PS, respectively.

Figure 4 shows SEM photographs of H-TiO_2 films. More than 20 layers of quasi-ordered spherical hollow shells were observed at some view points. The thickness of shell wall was *ca.* 10 nm. For the sample started from suspension containing A-PS and TALH 0.0025 mol dm^{-3}, the fcc configuration was observed especially on the surface in one to several millimeters range. However, the quasi-fcc ordered shells were discretely scattered on the substrate, and some parts of the substrate were not covered with films. On the other hand, although for the sample from C-PS the ordered structure was not observed (Fig. 4(d)) in micrometer view, the hollow shells smoothly coated almost all over the substrate. This more excellent dispersion by C-PS in appearance is due to uniform mixture of PS and

TALH in the precursor originating from their affinitive relationship. In both cases, there are observed many broken points of shells owing to PS-PS spheres contact at the initial precursor as shown in an inserted scheme in Fig. 4, leading to skeleton-like structure after calcinations.

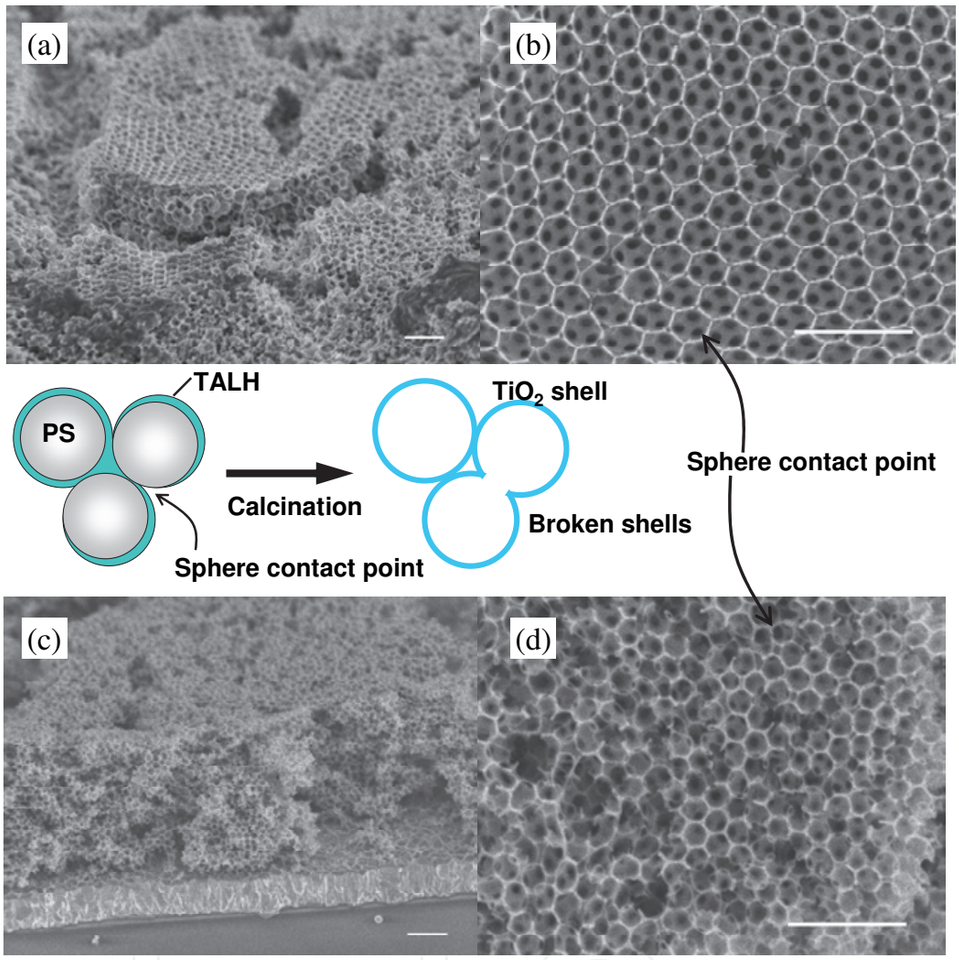

Fig. 4. Cross-sectional or suface SEM photographs of H-TiO_2 films on FTO substrates prepared from (a) or (b) A-PS and (c) or (d) C-PS, respectively. Scale bars correspond 1 μm.

Figure 5 shows XRD pattern of hollow shells film prepared on a quartz glass substrate by calcination of C-PS-TALH precursor. The pattern shows the TiO_2 shell film to be predominantly anatase type crystalline phase while the peaks were broad owing to nanocrystalline.(International Center for Diffraction Data, 1990)
The crystallite size (D) of the calcined film can be estimated from Scherrer's formula (Kim et al., 2008)

$$D = \frac{0.89\lambda}{\beta \cos\theta} \tag{1}$$

where λ is the wavelength of the X-ray, β is the peak width and θ is the Bragg angle of the peak.

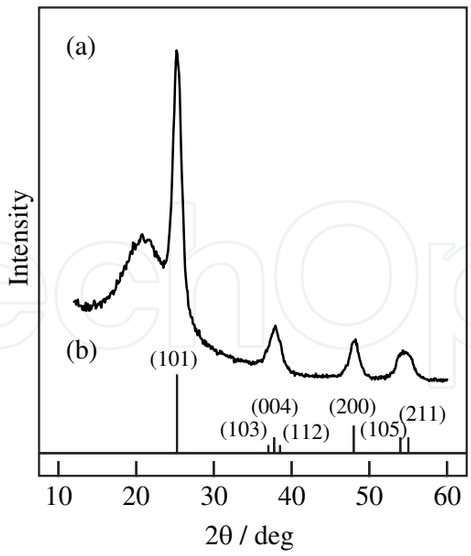

Fig. 5. XRD patterns of (a) H-TiO_2 film on quartz glass substrate and (b) an authentic pattern of anatase-type TiO_2.(International Center for Diffraction Data, 1990)

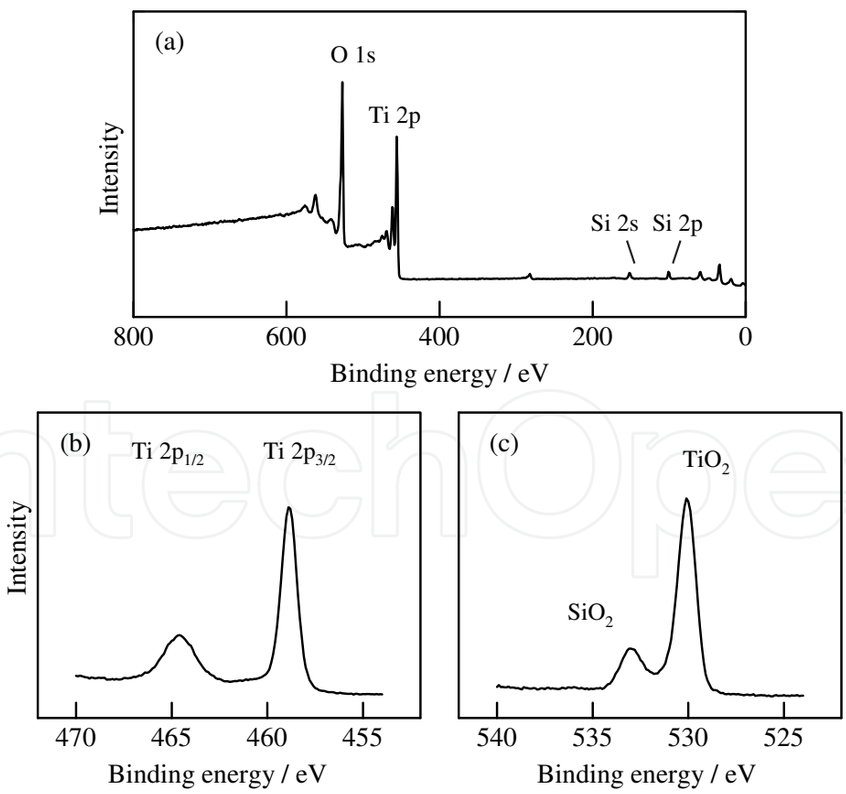

Fig. 6. XP spectra of hollow TiO_2 film on quartz glass substrate prepared from C-PS (0.28 %) and 0.005 mol dm^{-3} TALH; (a) wide scan spectrum, (b) Ti 2p and (c) O 1s photoelectron spectra.

On the hypothesis that the sample is constituted by isotropic and spherical crystallites, the width of the most intensive X-ray diffraction peak, corresponding to anatase (101) plane at 25.273°, is adopted for the calculation of the β value. With the β value: 0.0153 (radian) obtained after the exclusion of the effect of $K\alpha_2$ line and optical system of the instrument, the D value is estimated to be 7.7 nm.

Figure 6 shows XP spectra of the surface of hollow shells film. In the wide energy range spectrum (Fig. 6 (a)) small peaks of Si 2p and Si 2s photoelectron originating from quartz glass substrate were observed as well as main titanium and oxygen peaks. Almost identical peak positions (within 1 eV) of Ti $2p_{3/2}$ region spectrum for the film and standard TiO_2 (Chigane et al., 2009) at 458.9 and 458.7 eV, respectively, suggest that the chemical state of the hollow shells film can be assigned to TiO_2. The main peak and secondary peak at 530 eV and at around 533 eV in O 1s photoelectron region spectrum can be attributed to titanium oxide (Ti–O–Ti) and silica of substrate, respectively, from references. (Moulder et al., 1992)

Figure 7 shows optical properties of H-TiO_2 films prepared from C-PS and TALH.

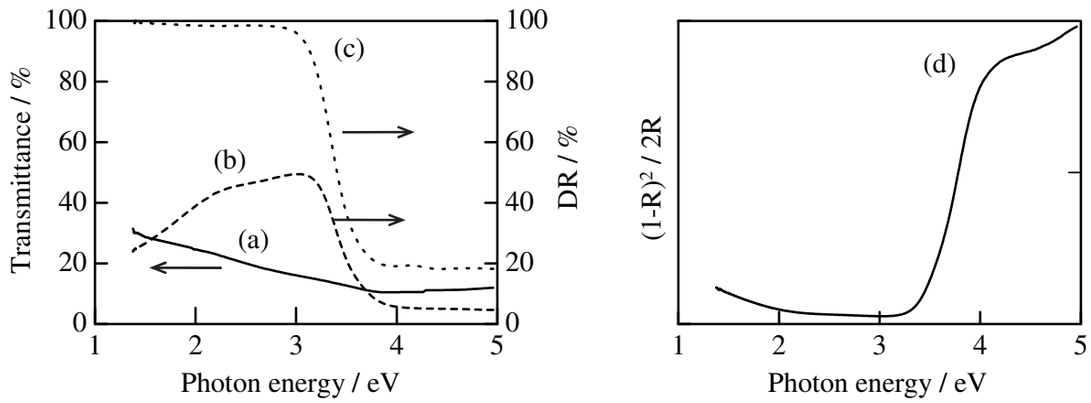

Fig. 7. Relationship between H-TiO_2 film on quartz glass substrate from C-PS-TALH and UV-visible photon energy: (a, solid line) transmission spectrum of the film and (b, dashed line) or (c, dotted line) diffuse reflection spectrum of film or powder sample, respectively and (d) Kubelka-Munk function plots for the powdered sample transformed from DR spectrum corresponding to (c).

Absence of clear attenuation dip in transmission spectrum indicates random configuration of hollow shells. Decrease and increase of transmittance and DR of film samples, respectively, according to photon energy up to ca. 3 eV are due to scattering of light by aggregation of TiO_2 hollows. Taking account of DR of powder sample the decrease of both transmittance and DR of film sample at higher than 3 eV are due to interband photo-absorption of TiO_2. Such change of DR of powder sample can be associated with absorption coefficient (α) using Kubelka-Munk function (Kortüm, 1969; Murphy, 2007)

$$F(R) = \frac{(1-R)^2}{2R} = \frac{\alpha}{S} \tag{2}$$

as shown in Fig. 7(d), where R and S indicate diffuse reflectance and scattering coefficient, respectively. Although all terms depend on energy (wavelength) of incident light, the sizes

of hollow shells collectives (more than 1 μm) are enough larger than wavelength and in the wavelength range between 310 nm (ca. 4 eV) and 410 nm (ca. 3 eV) concerning photoabsorption (Fig. 7(c)) the change of S value might be little. Therefore in relation to absorption S can be assumed to be constant and then we investigated band edge using α/S values. The relationship of α and photon energy (hν) of semiconductors near the absorption edge region for direct or indirect transition is given by

$$(\alpha h\nu)^2 = A(h\nu - E_g) \tag{3}$$

or

$$(\alpha h\nu)^{1/2} = A(h\nu - E_g) \tag{4}$$

respectively, where A and E_g are proportion constant and band gap energy.(Pankove, 1971) The linear relationship of Eq. (3) and (4) indicate that in the plots of $(\alpha h\nu)^2$ or $(\alpha h\nu)^{1/2}$ versus hν the optical band gap can be determined by intersection of extrapolated straight line with hν axis. (Barton et al., 1999; Han et al., 2007; Nowak et al., 2009) Based on above mentioned assumption we derived the optical band gaps as 3.5 eV and 3.2 eV from intersection points of linear fitting line with $(\alpha h\nu/S)^2$ and $(\alpha h\nu/S)^{1/2}$ versus hν for direct and indirect process, respectively, as shown in Fig. 8. At present we propose the latter value because 3.2 eV of E_g for anatase TiO_2 is commonly accepted.(O'Regan & Grätzel, 1991; Tang et al., 1994) However more investigation is necessary since it has not been clarified whether interband transition of anatase TiO_2 is direct or indirect. (Asahi et al., 2000; Mo & Ching, 1995)

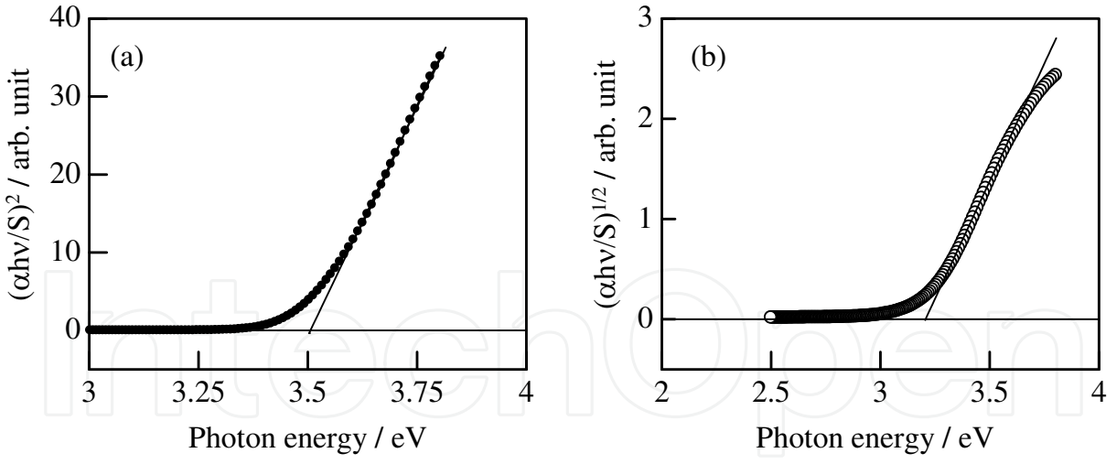

Fig. 8. Plots of (a) $(ahv/S)^2$ and (b) $(ahv/S)^{1/2}$ against UV-visible photon energy of powdered H-TiO_2 transferred from a / S spectrum corresponding to Fig. 7(d). Linear lines are drawn to determine band gap energies.

3.2 Enhanced film quality by electrodeposition

Figure 9(a) shows low magnification SEM image of the films indicating considerable volume change by calcination. After calcination the film was constricted and broken apart as expected in introduction section. Moreover maybe owing to the stress by crystallization and plastic strain the film easily detached from substrate. Such poor quality of the films and

large crack made us expect low utility for DSSC electrode. Figure 9(b) and (c) show SEM images of TiO_2-coated H-TiO_2 film by electrodeposition before calcination. Although on the top surface view some narrow cracks were observed within 1 μm width, recognition of only hollow spheres in the back of the cracks indicates that the FTO substrate are not exposed. Cross-sectional view shows hollow shells suggesting successful maintenance of PS-TALH structure during electrodeposition.

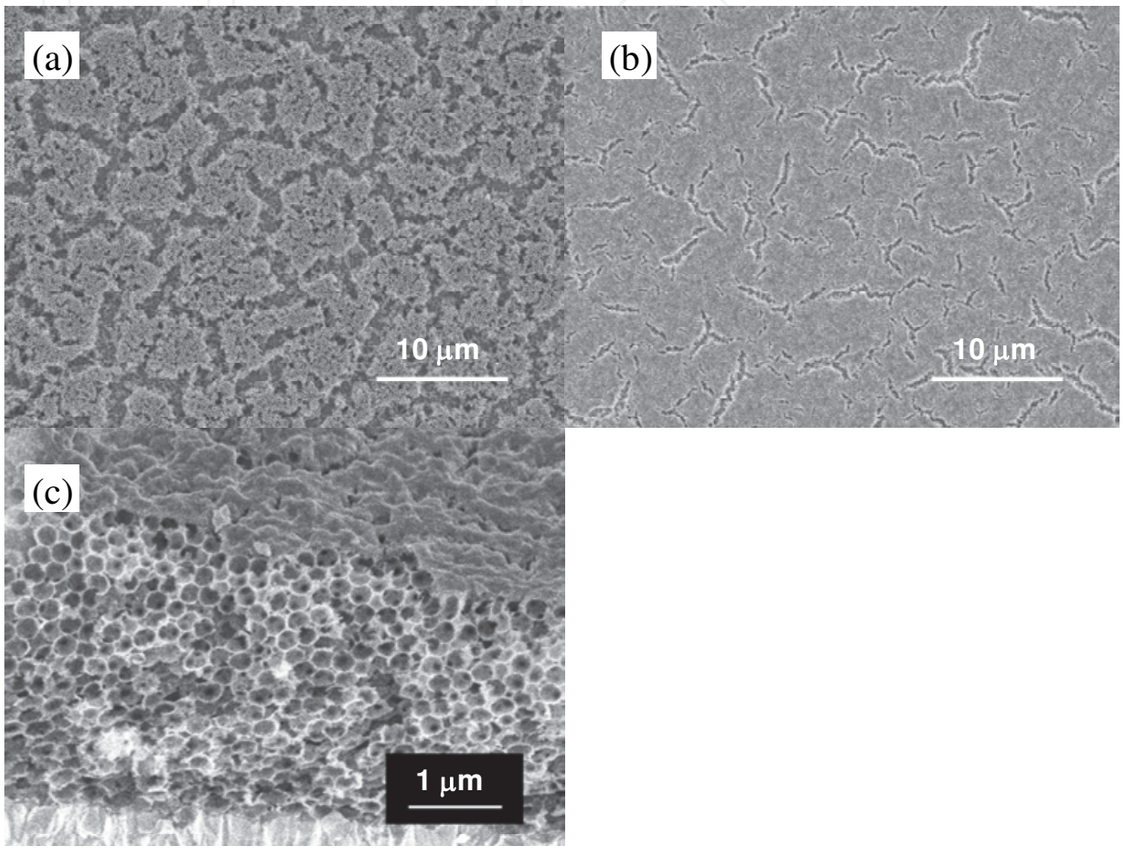

Fig. 9. SEM photographs of H-TiO_2 films on FTO substrates; (a) or (b) surface view of the film without or with electrodeposition TiO_x coating, respectively, and (c) cross-sectional view of the film with electrodeposition TiO_x coating. In both cases the precursors are C-PS-TALH.

3.3 DSSC properties

Figure 10 and Table 1 show typical results of DSSC assessment for three type TiO_2 electrodes. The conversion efficiency value of the cell using only H-TiO_2 electrode: 0.91 % (Fig. 10(a)) was about 4 times lower than that for the cell: 3.98 % using standard nc-TiO_2 electrode (Fig. 10(b)).

The conversion efficiency value of the cell using only H-TiO_2 electrode: 0.91 % (Fig. 10(a)) was about 4 times lower than that for the cell: 3.98 % using standard nc-TiO_2 electrode (Fig. 10(b)), despite 3.2 times smaller amount of TiO_2. There can be thought to be two reasons for such insufficient efficiency. One is lower short circuit current density (J_{SC}). The compli-cated morphology of hollow TiO_2 film might contribute to the increase of specific contact area

with dye molecules and to harvesting light by scattering in the hollow shells. However a large number of broken points in the skeleton structure and few contact points with substrate supposedly leaded poor conduction of photo-induced electrons. The other is lower open circuit voltage (V_{OC}) due to direct contact between electrolyte solution and FTO substrate through wider film crack points. So as to improve the two problems we inserted initial flat TiO_2 layer on the substrate by electrolysis of TALH solution. Remarkably improved DSSC performance: 2.90 % for the composite (C-TiO_2) film composed of electrodeposited TiO_2 bottom layer and hollow TiO_2 top layer has been shown (Fig. 10(c) and Table 1) compared with single hollow layer (0.91 %), including enhancement of V_{OC} and FF values. The area density of TiO_2 of nanoparticles electrode was as more than 2.4 times as the composite hollow shell film, whereas the change of the conversion efficiency was 1.4 times. This indicates the conversion efficiency per-TiO_2-weight for the composite hollow shell film is higher than nc-TiO_2 film owing to homogeneity effect of blocking layer making complicated structure of H-TiO_2 available

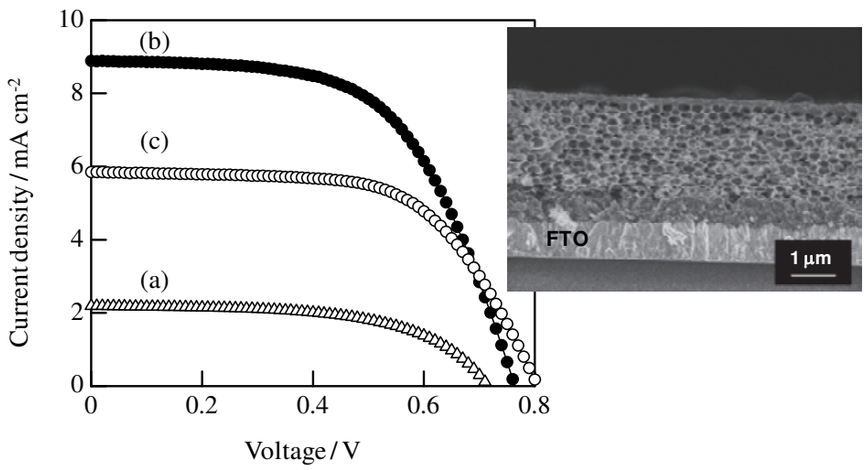

Fig. 10. Photocurrent density voltage curves of DSSCs using (a) H-TiO_2, (b) nc-TiO_2 and (b) C-TiO_2 film. The cross-sectional SEM photograph indicates the C-TiO_2 sample corresponding to curve (c).

TiO_2 films	Area density of TiO_2 / mg cm^{-2} (by XRF)	J_{SC} / mA cm^{-2} [a]	V_{OC} / V [b]	FF[c]	Eff / % [d]
Hollow shell	0.179	2.19	0.716	0.580	0.911
Composite	0.244	5.85	0.805	0.615	2.90
Nano-particles	0.587	8.89	0.763	0.585	3.98

[a]Short circuit current density. [b]Open circuit voltage. [c]Fill factor. [d]Conversion efficiency.

Table 1. DSSC properties of two TiO_2 film electrodes.

Figure 11 shows IPCE assessments of cells using three type TiO_2 electrodes: nc-TiO_2, simply electrodeposited TiO_2 (E-TiO_2) and C-TiO_2 film. In this comparison we electrodeposited thicker first film than that in above J-V characterization. By this effect the conversion efficiency of C-TiO_2 film was somewhat enhanced to 3.44 %. The normalized IPCE curves for the films (Fig. 11(e), (f), (g)) have shown good spectral accordance of photocurrent with

photoabsorption of dye (Fig. 10(d)). Moreover heightening of composite TiO_2 film (Fig. 11(f)) by 14 % and 11 % at 450 nm and 600 nm of wavelength, respectively, against simple electrodeposited film (Fig. 11(e)), proves wavelength-independent increase of photocurrent by the addition of hollow shells as top layer. This seems to arise simply from increase of amount of TiO_2 and to imply low optical effect of our hollow shells, remaining what should be improved.

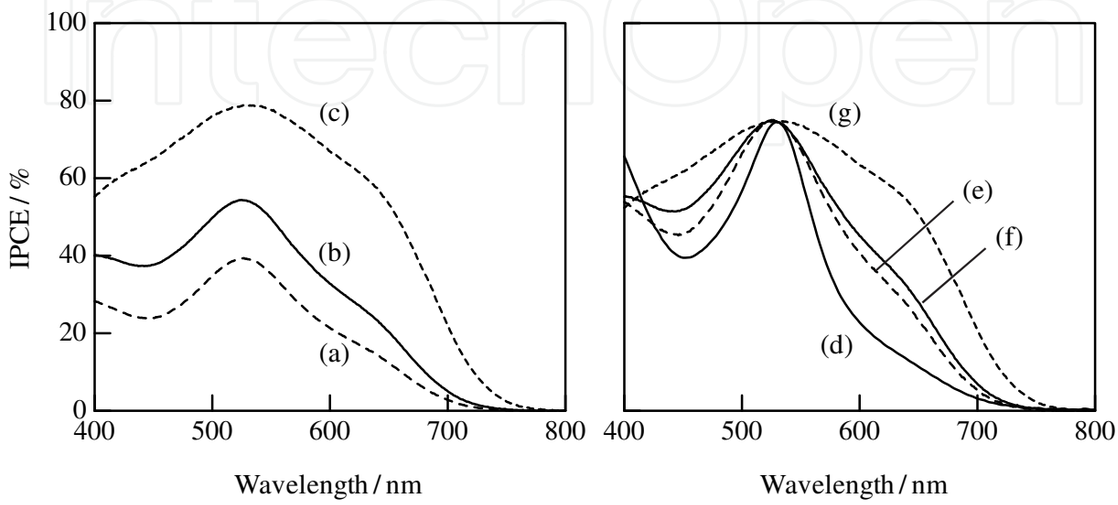

Fig. 11. IPCE spectra of DSSC using (a, dashed line) or (e, dashed line) E-TiO_2 film, (b, solid line) or (f, solid line) C-TiO_2 film and (c, dotted line) or (g, dotted line) nc-TiO_2 film.

4. Conclusions

Hollow TiO_2 (H-TiO_2) shell films have been prepared using environmentally benign Ti-lactate complex (TALH) as a titanium source. A precursor has been prepared from an aqueous colloidal suspension containing both polystyrene (PS) and TALH. Successive calcination of the PS-TALH precursor at 723 K led to the decomposition of PS and formation of hollow spherical shells. Employing PS with cationic surface functional group (C-PS) gave rise to smoothly spreading of hollow shells films in wider area compared with conventional PS possessing anionic groups (A-PS). The characterizations by X-ray diffraction and X-ray photoelectron spectroscopy have proved that the hollow shell films can be assigned to anatase TiO_2. Optical characteristics of H-TiO_2 films from C-PS-TALH have shown they are not in an inverse opal structure. Diffuse reflection spectroscopy combined with Kubelka-Munk treatment has revealed wide optical band gap as equal or more than 3.2 eV, indicating transparency of the films for visible light. It has been found that combination with electrodeposition of TiO_x films strongly supports quality and DSSC properties of H-TiO_2 films in two aspects. First the electrodeposition onto the PS-TALH precursor film effectively prevented widely cracking in the calcination process. Moreover the electrodeposition onto FTO substrate before H-TiO_2 layer, namely fabrication of composite film (C-TiO_2 film), substantially enhanced DSSC energy conversion efficiency: 2.9 % which was comparable to an electrode using commercially available TiO_2 nanocrystalline particle (nc-TiO_2). The IPCE curve of C-TiO_2 film has revealed the increase of photocurrent due to light-harvesting effect.

On the other hand its independence of wavelength has indicated that H-TiO_2 lacks photonic crystal effect and then a future investigation on improvement of arraying of H-TiO_2 is needed.

5. References

Asahi, R.; Taga, Y.; Mannstadt, W. & Freeman, A. J. (2000). Electronic and optical properties of anatase TiO_2, *Physical Review B*, Vol.61, No.11, pp 7459–7465, ISSN 1098-0121

Barton, D. G.; Shtein, M.; Wilson, R. D.; Soled, S. L. & Iglesia, E. (1999). Structure and Electronic Properties of Solid Acids Based on Tungsten Oxide Nanostructures, *Journal of Physical Chemistry B*, Vol.103, No.4, pp 630-640, ISSN 1520-6106

Bisquert, J.; Cahen, D.; Hodes, G.; Rühle, S. & Zaban, A. (2004). Physical Chemical Principles of Photovoltaic Conversion with Nanoparticulate, Mesoporous Dye-Sensitized Solar Cells, *Journal of Physical Chemistry B*, Vol.108, No.24, pp 8106–8118, ISSN 1520-6106

Caruso, F.; Shi, X.; Caruso, R. A. & Susha, A. (2001). Hollow Titania Spheres from Layered Precursor Deposition on Sacrificial Colloidal Core Particles, *Advanced Materials*, Vol.13, No.10, pp 740–744, ISSN 0935-9648

Chigane, M.; Watanabe, M.; Izaki, M.; Yamaguchi, I. & Shinagawa, T. (2009). Preparation of Hollow Titanium Dioxide Shell Thin Films by Electrophoresis and Electrolysis for Dye-Sensitized Solar Cells, *Electrochemical and Solid-State Letters*, Vol.12, No.5, pp E5–E8, ISSN 1099-0062

Enright, B. & Fizmaurice, D. (1996). Spectroscopic Determination of Electron and Hole Effective Masses in a Nanocrystalline Semiconductor Film, *Journal of Physical Chemistry*, Vol.100, No.3, pp 1027–1035, ISSN 0022-3654

Galusha, J. W.; Tsung, C-K.; Stucky, G. D. & Bartl, M. H. (2008). Optimizing Sol-Gel Infiltration and Processing Methods for the Fabrication of High-Quality Planar Titania Inverse Opals, *Chemistry of Materials*, Vol.20, No.15 pp 4925–4930, ISSN 0897-4756

Guldin, S.; Httner, S.; Kolle, M.; Welland, M. E.; Müller-Buschbaum, P.; Friend, R. H.; Steiner, U. & Ttreault, N. (2010). Dye-Sensitized Solar Cell Based on a Three-Dimensional Photonic Crystal, *Nono Letters*, Vol.10, No.7, pp 2303–2309, ISSN 1530-6984

Han, T. -Y.; Wu, C. -F. & Hsieh, C. -T. (2007). Hydrothermal synthesis and visible light photocatalysis of metal-doped titania nanoparticles, *Journal of Vacuum Science & Technology, B: Microelectronics and Nanometer Structures--Processing, Measurement, and Phenomena*, Vol.25, No.2, pp 430-435, ISSN 1071-1023

Hartsuiker, A. & Vos, W. L. (2008). Structural Properties of Opals Grown with Vertical Controlled Drying, *Langmuir*, Vol.24, No.9, pp 4670–4675, ISSN 0743-7463

International Center for Diffraction Data, Joint Committee on Powder Diffraction Standards, (1990). *Powder Diffraction File*, set 21, No.1272, Swarthmore, Pennsylvania, USA

Kang, S. H.; Choi, S-H.; Kang, M-S.; Kim, J-Y.; Kim, H-S.; Hyeon, T. & Sung, Y. -E. (2008). Nanorod-Based Dye-Sensitized Solar Cells with Improved Charge Collection Efficiency, *Advanced Materials*, Vol.20, No.1, pp 54–58, ISSN 0935-9648

Kang, T-S.; Smith, A. P.; Taylor, B. E. and Durstock, M. F. (2009). Fabrication of Highly-Ordered TiO_2 Nanotube Arrays and Their Use in Dye-Sensitized Solar Cells, *Nono Letters*, Vol.9, No.2, pp 601–606, ISSN 1530-6984

Karuppuchamy, S.; Amalnerkar, D. P.; Yoshida, T.; Sugiura, T. & Minoura, H. (2001). Cathodic electrodeposition of TiO_2 thin films for dye-sensitized photoelectrochemical applications, *Chemistry Letters*, Vol.30, No.1, pp 78-79, ISSN 0366-7022

Kim, G. -M.; Lee, S. -M.; Michler, G. H.; Roggendorf, H.; Gösele, U. & Knez, M. (2008). Nanostructured pure anatase titania tubes replicated from electrospun polymer fiber templates by atomic layer deposition, *Chemistry of Materials*, Vol.20, No.9, pp 3085-3091, ISSN 0897-4756

King, J. S.; Grangnard, E. & Summers, C. J. (2005). TiO_2 Inverse Opals Fabricated Using Low-Temperature Atomic Layer Deposition, *Advanced Materials*, Vol.17, No.8, pp 1010–1013, ISSN 0935-9648

Kondo, Y.; Yoshikawa, H.; Awaga, K.; Murayama, M.; Mori, T.; Sunada, K.; Bandow, S. & Iijima S. (2008). Preparation, Photocatalytic Activities, and Dye-Sensitized Solar-Cell Performance of Submicron-Scale TiO_2 Hollow Spheres, *Langmuir*, Vol.24, No.2, pp 547–550, ISSN 0743-7463

Kortüm, G. (1969). *Reflectance Spectroscopy*, pp 103-127, Springer-Verlag, ISBN 978-3540045872, New York, USA

Kwak, E. S.; Lee, W.; Park, N-G.; Kim, J. & Lee, H. (2009). Compact inverse-opal electrode using non-aggregated TiO_2 nanoparticles for dye-sensitized solar cells, *Advanced Functional Materials*, Vol.19, No.7, pp 1093–1099, ISSN 1616-301X

Liu, W.; Zou, B.; Zhao, J. & Cui, H. (2010). Optimizing sol-gel infiltration for the fabrication of high-quality titania inverse opal and its photocatalytic activity, *Thin Solid Films*, Vol.518, No.17, pp 4923–4927, ISSN 0040-6090

Mo, S. –D. & Ching, W. Y. (1995). Electronic and optical properties three phases of titanium dioxide: Rutile, anatase, and brookite, *Physical Review B*, Vol.51, No.19, pp 13023–13032, ISSN 1098-0121

Moulder, J. F.; Stickle, W. F.; Sobol P. E. & Bomben, K. D. (1992). *Handbook of X-ray Photoelectron Spectroscopy*, Perkin-Elmer, p. 45, ISBN 0-9627026-2-5, Minnesota, USA

Murphy, A. B. (2007). Band-gap determination from diffuse reflectance measurements of semiconductor films, and application to photoelectrochemical water-splitting, *Solar Energy Materials and Solar Cells*, Vol.91, No.14, pp 1326-1337, ISSN 0927-0248

Nazeeruddin, M. K.; Péchy, P.; Renouard, T.; Zakeeruddin, S. M.; Humphry-Baker, R.; Comte, P.; Liska, P.; Cevey, L.; Costa, E.; Shklover, V.; Spiccia, L.; Deacon, G. B.; Bignozzi, C. A. & Grätzel, M. (2001). Engineering of Efficient Panchromatic Sensitizers for Nanocrystalline TiO_2-Based Solar Cells, *Journal of the American Chemical Society*, Vol.123, No.8, pp 1613–1624, ISSN 0002-7863

Nishimura, S.; Shishido, A.; Abrams, N. & Mallouk, T. E. (2002). Fabrication technique for filling-factor tunable titanium dioxide colloidal crystal replicas, *Applied Physics Letters*, Vol.81, No.24, pp 4532–4534, , ISSN 0003-6951

Nishimura, S.; Abrams, N.; Lewis, B. A.; Halaoui, L. I.; Mallouk, T. E.; Benkstein, K. D.; van de Lagemaat, J. & Frank, A. J. (2003). Standing Wave Enhancement of Red

Absorbance and Photocurrent in Dye-Sensitized Titanium Dioxide Photoelectrodes Coupled to Photonic Crystals, *Journal of the American Chemical Society*, Vol.125, No.20, pp 6306–6310, ISSN 0002-7863

Nowak, M.; Kauch, B. & Szperlich, P. (2009). Determination of energy band gap of nanocrystalline SbSI using diffuse reflectance spectroscopy, *Review of Scientific Instruments*, Vol.80, No.4, pp 046107-1-046107-3, ISSN 0034-6748

O'Regan, B. & Grätzel, M. (1991). A low-cost, high-efficiency solar cell based on dye-sensitized colloidal TiO_2 films, *Nature*, Vol.353, No.6346, pp. 737–740, ISSN 0028-0826

Pankove, J. I. (1971). *Optical processes in semiconductors*, pp 34-42, Dover Publications, ISBN 0-486-60275-3, New York, USA

Paulose, M.; Shankar, K.; Varghese, O. K.; Mor, G. K. & Grimes, C. A. (2006). Application of highly-ordered TiO_2 nanotube-arrays in heterojunction dye-sensitized solar cells, *Journal of Physics D: Applied Physics*, Vol.39, No.12, pp 2498–2503, ISSN 0022-3727

Peng, T. Y.; Hasegawa, A.; Qui, J. R. & Hirao, K. (2003). Fabrication of Titania Tubules with High Surface Area and Well-Developed Mesostructural Walls by Surfactant-Mediated Templating Method, *Chemistry of Materials*, Vol.15, No.10, pp 2011–2016, ISSN 0897-4756

Qi, L.; Sorge, J. D.; & Birnie III, D. P. (2009). Dye-sensitized solar cells based on TiO_2 coatings with dual size-scale porosity, *Journal of the American Ceramic Society*, Vol.92, No.9, pp 1921–1925, ISSN 0002-7820

Rouse, J. H. & Ferguson, G. S. (2002). Stepwise Formation of Ultrathin Films of a Titanium (Hydr) Oxide by Polyelectrolyte-Assisted Adsorption, *Advanced Materials*, Vol.14, No.2, pp 151–154, ISSN 0935-9648

Ruani, G.; Ancora, C.; Corticelli, F.; Dionigi, C. & Rossi, C. (2008). Single-step preparation of inverse opal titania films by the doctor blade technique, *Solar Energy Materials and Solar Cells*, Vol.92, No.5, pp 537–542, ISSN 0927-0248.

Tachibana, Y.; Moser, J. E.; Grätzel, M.; Klug, D. R. & Durrant, J. R. (1996). Subpicosecond Interfacial Charge Separation in Dye-Sensitized Nanocrystalline Titanium Dioxide Films, *Journal of Physical Chemistry*, Vol.100, No.51, pp 20056–20062, ISSN 0022-3654

Tang, H.; Prasad, K.; Sanjinès, R.; Schmid, P. E. & Lévy, F. (1994). Electrical and optical properties of TiO_2 anatase thin films, *Journal of Applied Physics*, Vol.75, No.4, pp 2042-2047, ISSN 0021-8979

Watanabe, M.; Aritomo, H.; Yamaguchi, I.; Shinagawa, T.; Tamai, T.; Tasaka, A. & Izaki, M. (2007). Selective Preparation of Zinc Oxide Nanostructures by Electrodeposition on the Templates of Surface-functionalized Polymer Particles, *Chemistry Letters*, Vol.36, No.5, pp 680–681, ISSN 0366-7022

Yamaguchi, K.; Sawatani, S.; Yoshida, T.; Ohya, T.; Ban, T.; Takahashi Y. & Minoura, H. (2005). Electrodeposition of TiO_2 thin films by anodic formation of titanate/benzoquinone hybrid, *Electrochemical and Solid-State Letters*, Vol.8, No.5, pp C69-C71, ISSN 1099-0062

Yang, S-C.; Yang, D-J.; Kim, J.; Hong, J-M.; Kim, H-G.; Kim, I-D. & Lee, H. (2008). Hollow TiO_2 Hemispheres Obtained by Colloidal Templating for Application in Dye-

Sensitized Solar Cells, *Advanced Materials*, Vol.20, No.5, pp 1059–1064, ISSN 0935-9648

Ye, Y. -H.; LeBlanc, F.; Hache, A.; Truong, V. -V. (2001). Self-assembling three-dimensional colloidal photonic crystal structure with high crystalline quality, *Applied Physics Letters*, Vol.78, No.1, pp 52-54, ISSN 0003-6951

Yip, C. -H.; Chiang, Y. -M. & Wong, C. -C. (2008). Dielectric Band Edge Enhancement of Energy Conversion Efficiency in Photonic Crystal Dye-Sensitized Solar Cell, *Journal of Physical Chemistry C*, Vol.112, No.23, pp 8735–8740, ISSN 1932-7447

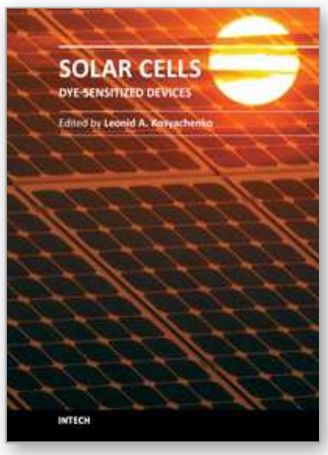

Solar Cells - Dye-Sensitized Devices
Edited by Prof. Leonid A. Kosyachenko

ISBN 978-953-307-735-2
Hard cover, 492 pages
Publisher InTech
Published online 09, November, 2011
Published in print edition November, 2011

The second book of the four-volume edition of "Solar cells" is devoted to dye-sensitized solar cells (DSSCs), which are considered to be extremely promising because they are made of low-cost materials with simple inexpensive manufacturing procedures and can be engineered into flexible sheets. DSSCs are emerged as a truly new class of energy conversion devices, which are representatives of the third generation solar technology. Mechanism of conversion of solar energy into electricity in these devices is quite peculiar. The achieved energy conversion efficiency in DSSCs is low, however, it has improved quickly in the last years. It is believed that DSSCs are still at the start of their development stage and will take a worthy place in the large-scale production for the future.

INTECH
open science | open minds

InTech Europe
University Campus STeP Ri
Slavka Krautzeka 83/A
51000 Rijeka, Croatia
Phone: +385 (51) 770 447
Fax: +385 (51) 686 166
www.intechopen.com

InTech China
Unit 405, Office Block, Hotel Equatorial Shanghai
No.65, Yan An Road (West), Shanghai, 200040, China
中国上海市延安西路65号上海国际贵都大饭店办公楼405单元
Phone: +86-21-62489820
Fax: +86-21-62489821

IntechOpen